International Journal of Pavement Engineering

ISSN: 1029-8436 (Print) 1477-268X (Online) Journal homepage: http://www.tandfonline.com/loi/gpav20

Viscoelastic behaviour of asphalt modified by grafted tri-block copolymers: predictions of fractional rheological models

Maria A. Vargas, Antonio Sánchez, Gisela Guthausen & Octavio Manero

To cite this article: Maria A. Vargas, Antonio Sánchez, Gisela Guthausen & Octavio Manero (2015) Viscoelastic behaviour of asphalt modified by grafted tri-block copolymers: predictions of fractional rheological models, International Journal of Pavement Engineering, 16:8, 730-744, DOI: 10.1080/10298436.2014.953501

To link to this article: http://dx.doi.org/10.1080/10298436.2014.953501

International Journal of Pavement Engineering, 2015
Vol. 16, No. 8, 730–744, http://dx.doi.org/10.1080/10298436.2014.953501

Viscoelastic behaviour of asphalt modified by grafted tri-block copolymers: predictions of fractional rheological models

Maria A. Vargas[a]*, Antonio Sánchez[a], Gisela Guthausen[b] and Octavio Manero[a]

[a]*Instituto de Investigaciones en Materiales, Universidad Nacional Autónoma de México, A.P. 70-360, México, D.F. 04510, México;* [b]*KIT ITPC, 76131 Karlsruhe, Germany*

(*Received 11 January 2013; accepted 9 July 2014*)

Blends of asphalt with three maleic anhydride-modified triblock copolymers are prepared and analysed in detail for potential use in pavement construction. These blends are compared with those made with the copolymers without chemical modification. The use of grafted polymers improves the conventional properties of blends made with the asphalt and precursor polymers, such as penetration, softening point, storage stability at high temperature and the rheological properties. In addition, blends made with the chemically modified polymers present biphasic morphology with improved dispersion and interconnected phases. Semi-empirical models corresponding to a constitutive equation with fractional derivatives are proposed to predict the linear viscoelastic properties of the blends using few parameters for each temperature. The fractional Kelvin, fractional standard linear solid and fractional Maxwell models are shown to predict appropriately the linear viscoelastic properties from 25 to 75°C at frequencies from 0.1 to 100 rad/s.

Keywords: asphalt; grafted polymer; fractional rheological models; morphology; viscoelasticity

1. Introduction

Asphalt presents a viscoelastic behaviour and is commonly used in paved roads, adhesives and in other extensive applications (Brûle 1996, Lu and Isacsson 1997, Navarro *et al.* 2002, Airey *et al.* 2003, Becker *et al.* 2003, Polacco *et al.* 2006). It is composed of two main chemical species; namely, maltenes (saturated compounds, resins and aromatics) and asphaltenes (Lesueur and Gerard 1996, Navarro *et al.* 2001, 2007, Airey *et al.* 2003, Polacco *et al.* 2004a, 2004b, Airey *et al.* 2008). The limitations of asphalt in the paving industry are due to its intrinsic properties and inherent weakness that make the maintenance of a pavement system difficult and expensive. To improve asphalt properties, blends with a variety of polymeric compounds are made to enhance pavement performance and reduce different types of pavement distress, of which rutting, low-temperature cracking, load-associated fatigue cracking, stripping and hardening are commonly observed (Kraus and Rollmam 1980, Kraus 1982, Collins and Mikols 1985, Brûle *et al.* 1988, Collins and Bouldin 1992, Becker *et al.* 2003). Polymer-modified asphalts (PMAs) production involves physical mixing or chemical reactions *in situ* (Polacco *et al.* 2004a, 2004b, Mohammad *et al.* 2006, Vargas *et al.* 2009).

Reactive polymers are capable of forming chemical bonds with some asphalt molecules, improving the mechanical behaviour, storage stability and temperature susceptibility of the resulting blend (Fu *et al.* 2007, Kang *et al.* 2010, Cong *et al.* 2011). For instance, the production of asphalt with grafted polymers implies a curing process after mixing, coinciding with the storage stage of the material at high temperatures and long periods (Polacco *et al.* 2004a, 2004b). During this process, the functional groups of the polymer may react with the carboxylic groups of asphaltenes to form esters (Becker *et al.* 2003), improving dispersion thus inducing compatibility among phases. Due to the complex composition of asphalt, it is difficult to determine the amount and type of reactions occurring during the curing process (Fu *et al.* 2007, Cong *et al.* 2011). Linear viscoelastic properties of modified asphalts are strongly dependent on the changes in the composition, molecular weight distribution and, when considering multiphase systems, interface characteristics. In the rheological tests performed in the dynamic mode, data are taken in the range of deformation corresponding to linear viscoelastic behaviour and are generally expressed by master curves using the time–temperature superposition principle (TTSP). Some authors suggest that TTSP does not apply to asphalt at high temperatures or in some extreme cases when the asphalt presents highly crystalline fractions and high asphaltene contents (Lesueur and Gerard 1996), even in polymer-modified asphalts (Polacco *et al.* 2006). Several models have been proposed to describe asphalt viscoelasticity and most of them rely on the plot of master curves. They imply that TTSP holds for asphalt (Stastna *et al.* 1994, Lesueur and Gerard 1996, Da Silva *et al.* 2004, Polacco *et al.* 2004a, 2004b, Navarro *et al.* 2005, Mun and Zi 2010).

*Corresponding author. Email: angelesvh@yahoo.com

Systematic analysis of the rheological properties of the blends analysed in this work includes those using fractional calculus, the so-called fractional rheological models. The basic definitions of fractional calculus and combinations of fractional dashpots and springs, analogous to the mechanical representations of linear viscoelastic models (Friedrich 1991, Heymans and Bauwens 1994, Heymans 1996, Hernández Jiménez *et al.* 2002, Lewandowski and Chorazyczewski 2010, Papoulia *et al.* 2010), are considered in the analysis of the fractional Maxwell model (FMM), the fractional Kelvin model (FKM) and the fractional standard linear solid (FSLS). The advantage of fractional models is the ability to model the material behaviour over a wide range of frequencies at different temperatures with a small number of model parameters.

This work aims to compare the rheological properties of two asphalt modifiers (non-grafted tri-blocks and maleic anhydride (MAH)-grafted tri-block copolymers) and to describe predictions of the rheological properties of the blends by fractional rheological models.

2. Theory: rheological models

2.1 *Fractional Maxwell model*

Viscoelastic models containing fractional derivatives of different orders and other fractional operators with more than one independent fractional parameter have attracted considerable attention. This is due to fact that such models enable the description of rheological properties over a wide range of frequencies, and more importantly, provides remarkable agreement with experimental data (Rossikhin and Shitikova 2001).

FMM consists of a fractional dashpot with viscosity η and the fractional exponent α in series with a linear spring with modulus G_0 (Figure 1(a)). The total deformation or strain ε is the sum of the elastic and inelastic parts, i.e.:

$$\sigma + \tau_R^{\alpha} D_t^{\alpha} \sigma = \eta D_t^{\alpha} \varepsilon, \tag{1}$$

$$\text{where } \tau_R^{\alpha} = \eta / G_0 \text{ is the relaxation time}, \quad \alpha \neq 0, \tag{2}$$

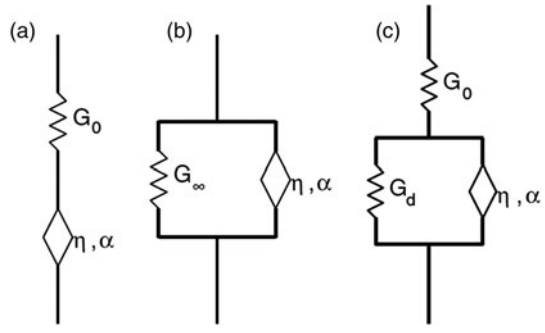

Figure 1. Schematic diagrams of three compound fractional elements (a) FMM, (b) FKM and (c) FSLS (Papoulia *et al.* 2010).

σ is the stress and D_t^{α} is the fractional time derivative of strain ε and stress σ, respectively.

By Fourier transformation of Equation (1), the expression for the complex modulus can be obtained (Rossikhin and Shitikova 2001, Hernández Jiménez *et al.* 2002, Lewandowski and Chorazyczewski 2010):

$$G^*(i\omega) = \eta \frac{(i\omega)^{\alpha}}{1 + \tau_R^{\alpha}(i\omega)^{\alpha}} \tag{3}$$

whose real and imaginary parts are the storage and loss moduli G' and G'', respectively.

$$G'(\omega) = \frac{\eta\omega^{\alpha}\cos(\pi\alpha/2) + \eta\tau_R\omega^{2\alpha}}{1 + 2\tau_R\omega^{\alpha}\cos(\pi\alpha/2) + \tau_R^2\omega^{2\alpha}}, \tag{4}$$

$$G''(\omega) = \frac{\eta\omega^{\alpha}\sin(\pi\alpha/2)}{1 + 2\tau_R\omega^{\alpha}\cos(\pi\alpha/2) + \tau_R^2\omega^{2\alpha}}. \tag{5}$$

Clearly, if $\alpha \to 1$, Equations (1), (4) and (5) reduce to the well-known expressions of the linear Maxwell model.

2.2 *Fractional Kelvin model*

FKM is represented by a parallel arrangement of a fractional dashpot, characterised by a viscosity η (with fractional exponent α) and a spring with modulus G_∞ (see Figure 1(b)). The governing equation is (Papoulia *et al.* 2010)

$$\sigma = G_\infty \varepsilon + \eta D^{\alpha} \varepsilon. \tag{6}$$

This equation can be solved along with the following function for the modulus, which interestingly presents a time-dependent relaxation function:

$$G(t) = G_\infty + \frac{G_\infty \tau_C^{\alpha}}{\Gamma(1-\alpha)t^{\alpha}}, \tag{7}$$

where $\tau_C^{\alpha} = \eta / G_\infty$ is the characteristic retardation time within FKM. When $\alpha \to 1$, the classical Kelvin model is obtained, which does not include a relaxation process, i.e. $G(t) = G_\infty$. The storage and loss moduli in this case are

$$G'(\omega) = G_\infty + \eta\omega^{\alpha}\cos(\pi\alpha/2), \tag{8}$$

$$G''(\omega) = \eta\omega^{\alpha}\sin(\pi\alpha/2). \tag{9}$$

2.3 *Fractional standard linear solid*

Another fractional model used for the description of viscoelastic materials is represented by a parallel arrangement of a spring with modulus G_d and a fractional dashpot with constants η and α. This arrangement is placed in series with another spring with modulus G_0

(Figure 1(c)). The governing equation is (Hernández Jiménez *et al.* 2002, Papoulia *et al.* 2010)

$$\sigma + \tau_R^{\alpha} D^{\alpha}\sigma = G_R\left(1 + \tau_C^{\alpha} D^{\alpha}\right)\varepsilon. \tag{10}$$

with

$$G_R = \frac{G_0 G_d}{G_0 + G_d},\quad \tau_R^{\alpha} = \tau_C^{\alpha}\frac{G_d}{G_0 + G_d},\quad \tau_C^{\alpha} = \frac{\eta}{G_d}. \tag{11}$$

The moduli are expressed as follows:

$$G'(\omega) = \frac{B + (C + AB)\omega^{\alpha}\cos(\pi\alpha/2) + AC\omega^{2\alpha}}{1 + 2A\omega^{\alpha}\cos(\pi\alpha/2) + A^2\omega^{2\alpha}}, \tag{12}$$

$$G''(\omega) = \frac{(C - AB)\omega^{\alpha}\sin(\pi\alpha/2)}{1 + 2A\omega^{\alpha}\cos(\pi\alpha/2) + A^2\omega^{2\alpha}}, \tag{13}$$

$$A = \frac{\eta}{G_0 + G_d},\quad B = G_R = \frac{G_0 G_d}{G_0 + G_d},\quad C = \frac{\eta G_0}{G_0 + G_d}. \tag{14}$$

If $G_d \to 0$, then $B = 0$, $A = \eta/G_0$ and $C = \eta$, and FMM (Equations (4) and (5)) is recovered.

3. Experimental

3.1 *Materials*

Asphalt AC-20 is the base material and was obtained from PEMEX, Mexico City, Mexico. Physical properties of this asphalt are as follows: penetration, 62 mm (25°C, ASTM standard D5); softening point, 48°C (ASTM standard D36); and a composition of 80% maltenes and 20% asphaltenes (on the basis of solubility in *n*-heptane; ASTM D3279-90).

The polymers used for asphalt additives, styrene-butadiene-styrene triblock copolymer (SBS) (Kraton D1101, Shell, Mexico City, Mexico), styrene-ethylene/butene-styrene triblock copolymer (SEBS) (Kraton G-1652, Shell Chemical, Co.), SEBS-g-MAH (Kraton G-1901X, Shell Chemical, Co.) and styrene-isoprene-styrene triblock copolymer (SIS) (Kraton 1124, Shell Chemical, Co.), were provided by Chemcentral, Mexico City, Mexico, and used as received. Polymer properties are disclosed in Table 1. SEBS-g-MAH contains 2 wt% MAH (Vargas *et al.* 2009).

SBS and SIS were grafted using reactive extrusion with MAH in a twin-screw conical counter-rotating Haake Rheocord Extruder 90, with an *L*/*D* ratio of 24:1, working at a rotational speed of 70 rpm (Sánchez Solís *et al.* 2000). Benzoil peroxide was used as an initiator at 160°C and the percentage of grafting was determined by thermogravimetric analysis in a high-resolution TA Instruments Q500HR (New Castle, USA) equipment under nitrogen atmosphere, with temperature ramps of 10 and 5°C/min. Calibration was made with Alumel and Niquel (Curie temperature); see Table 1.

3.2 *Preparation of the modified asphalt*

In stainless steel containers, 200 g of asphalt and 4 wt% of each polymer were placed at 180°C and 500 rpm stirring for 4 h. The modified asphalt was prepared under nitrogen atmosphere to avoid degradation. To exclude the effect of asphalt ageing during the mixing process to evaluate accurately the presence of polymer and its effects, the base asphalt (blank sample) was obtained under the same conditions as the modified blends. Slight differences among the values of both viscoelastic functions for pure asphalt and blank sample of asphalt were observed.

3.3 *Characterisation of polymers*

The differential scanning calorimetry (DSC) analyses were carried out in DSC Q100 and DSC 2910 equipments (TA Instrument, New Castle, USA). The calibration was made with Hg and In. Heating and cooling thermograms were carried out at the standard rate of 10°C/min from −130 to 130°C under nitrogen atmosphere. Only the second run was considered. Results are shown in Table 1.

Gel permeation chromatography (GPC) data for copolymers were carried out with an Alliance Separation Module HPLC-GPC Waters 2695, two columns Waters (Milford, MA, USA) HSP gel: HR MB-L with M_w ranging from 5×10^2 to 7×10^5 and HR MB-M with M_w ranging from 1×10^3 to 4×10^6 with dimensions of 150 mm × 6.0 mm. Column temperature was controlled by an oven at 33°C. Tetrahydrofuran (THF) flow velocity was 0.5 ml/min, injection volume was 10 µl and analysis time was 20 min for each sample. THF was previously filtered using a porous membrane with a pore size of 0.45 µm. The HPLC-GPC equipment was coupled online to the

Table 1. Properties of triblock polymers and grafted polymers.

Polymer	Styrene (%)	Structure	MAH (%)	$T_{g,PS}$ (°C)	$T_{g,PMID}$ (°C)	$\Delta H_{Tm\beta}$ (J/g)	$M_w \times 10^4$ (g/mol)	*D*
SBS	30	Linear	–	92	−89	–	7.133	1.096
SIS	30	Radial	–	90	−74	–	8.168	1.038
SEBS	30	Linear	–	70	−72	10	7.166	1.086
SBS-g-MAH	30	Linear	0.4	92	−86	–	8.207	1.210
SIS-g-MAH	30	Radial	0.8	87	−65	–	9.468	1.820
SEBS-g-MAH	30	Linear	2	65	−61	8.7	9.184	1.283

following detectors at 35°C: multi-angle light-scattering photometer (MALS (Agilent Technologies, Mexico City, Mexico), Dawn EOS (Wyatt Technology, Santa Barbara, CA, USA)) with 16 angles, from 12.5° to 164.9°; a ViscoStar viscometer that measures the pressure drop in four capillaries and an Optilab-rEX interferometer for concentration determinations. The refraction index increment (d*n*/d*c*) is measured with an OptiLab-rEX device at a wavelength of 685 nm. A linear column (ultra styragel, Waters) was calibrated using a series of narrow polystyrene (PS) standards having M_w ranging from 1700 to 4,200,000. Molecular weights (M_w) and polydispersity (D) are shown in Table 1.

3.4 *Characterisation of asphalt blends*

To characterise the properties of the asphalt, conventional test methods such as penetration test and softening point test were performed. Results are shown in Table 2.

The stability tests were performed in aluminium-covered glass tubes of 3.5 cm diameter and 19 cm height under nitrogen atmosphere. They were placed in an oven at 180°C for 3 days in vertical position (Lu and Isacsson 1997, Becker *et al.* 2003). The PMA sample was cooled to room temperature and thereafter it was cut into three parts. The softening temperature test was applied to the upper and lower sections of each sample. They were also characterised using rheometry to evaluate the separation index (I_S). Differences observed in the softening point of the upper and lower sections indicate the degree of heterogeneity of the blend caused by polymer migration to the surface (Lu and Isacsson 1997). If the difference is lower than 2.5°C, stability is considered adequate.

Polymer distribution in the PMA macro-phase was observed by fluorescence microscopy using a Carl-Zeiss KS 300 microscope at ambient temperature with a wavelength of 390–450 nm at 20× magnification. Micrographs were taken with a MC100 camera equipped with an automatic counter. The polymer-rich phase appeared white while the asphalt-rich phase was dark. For the morphological analysis, asphalt samples were taken during the PMA preparation, directly from the mixing can and poured into small cylindrical moulds (1 cm diameter, 2 cm height). To preserve the instantaneous morphology, the moulds were preheated up to the mixing temperature so that the asphalt was not subjected to quenching when in contact with the metal. The moulds were placed in an oven at 180°C for 15 min and cooled to room temperature. Results indicate that the fundamental properties and morphology of the modified asphalt are only dependent on the type of polymer.

The rheological properties of samples were measured using a controlled stress AR-1000-N rheometer (TA Instrument, New Castle, USA) with the parallel plate fixture (25 mm diameter). Steady simple shear and small-amplitude oscillatory tests were performed. The temperature range covered from 25 to 75°C with 2°C increments keeping the strain for each temperature within the linear viscoelastic region in the oscillatory tests. The frequency varied from 0.1 to 100 rad/s at a constant temperature and strain. A stabilisation time of 15 min was allowed for each sample.

4. Results and discussion

4.1 *Polymer modified asphalts*

The grafted polymers used in the modification of asphalt AC-20 present different MAH contents (Table 1). As mentioned in Section 3.1, SEBS-g-MAH was a commercial polymer, while SBS-g-MAH and SIS-g-MAH were grafted using reactive extrusion with MAH and benzoil peroxide under same reaction conditions (Sánchez Solís *et al.* 2000). We should assume that the differences in MAH content in SBS-g-MAH (0.4 wt%) and SIS-g-MAH (0.8 wt%) are due to polyolefin molecular structure and molecular weight, leading to different reaction pathways, the level of grafted functionality, the extent and type of any side reaction (Moad 1999, Machado *et al.* 2001, Aimin and Chao 2003, Nakason *et al.* 2004) or simply differences in mixing efficiency or parameters such as the melt temperature in reactive extrusion. It is well known that in polyolefins, several structurally different radical sites can be produced by the action of radical initiators. The predominantly secondary and tertiary macroradicals have different reactivities towards MAH (Heinen *et al.* 1996). The effect of polyolefin composition on MAH grafting is still not fully understood, due to the lack of insight into the reaction mechanism. Grafting reactions involve initiation

Table 2. PMA properties and softening point at the top and bottom sections of the blends.

Material	$T_{R\&B}$ (°C)	Penetration (dmm)	Top section (°C)	Bottom section (°C)	Difference (°C)	I_S
Asphalt	48	62	–	–	–	–
Asphalt/SBS	58	51	64	50	14	1.7410
Asphalt/SIS	65	47	68	60	8	1.5462
Asphalt/SEBS	67	45	65	58	7	1.4024
Asphalt/SBS-g-MAH	62	46	64	58	6	1.4885
Asphalt/SIS-g-MAH	72	40	72	70	2	0.6056
Asphalt/SEBS-g-MAH	68	42	68	63	5	0.7327

to form macro-radicals by subtraction of hydrogen atoms from the polymer chain through the initiator radicals, and addition of the unsaturated monomer to the macro-radicals (Qiu *et al.* 2005). Depending on the polyolefin composition (butadiene or isoprene), grafting occurs on the secondary or tertiary carbons. When long methylene sequences are present, reaction mainly occurs on the secondary carbons. If peroxide is used as the initiator (benzoil peroxide), cross-linking or chain scission ensue simultaneously with the grafting reaction. For this reason, the main reactions were controlled carefully to eliminate the side reactions (Moad 1999). There is evidence that SIS-g-MAH does not present chain scission, because its molecular weight does not decrease at the grafting site. Dharmarajan *et al.* (1995) found that most of the polypropylene has only a single MAH graft per polymer molecule. In general, the inter-chain compositional distribution of the anhydride groups is not uniform because a significant amount of highly functionalised oligomeric fraction should be present. On the other hand, the level of grafted MAH was controlled to avoid the production of gel fractions in the copolymer. The gel fractions in the copolymer induce swelling that prevents dissolution in organic solvents or maltenes (Jiang and Wilkie 1997). For this reason, SBS-g-MAH and SIS-g-MAH have less than 1.0 wt% of MAH content. The grafted MAH content in SBS, SIS or SEBS should have large effects on the rheological properties, thermal stability and compatibility of the modified asphalt. This effect is analysed in this work.

4.2 *Conventional asphalt tests: penetration and softening temperature*

In Table 2, the softening temperature increases and penetration decreases in the blends prepared with the grafted polymers with respect to the non-grafted systems are shown. The asphalt/SIS-g-MAH blend shows the highest softening point and lowest penetration, implying a rigidity increase and lesser susceptibility to permanent deformation.

4.3 *Fluorescence microscopy*

Polymer and asphalt are immiscible systems because of their chemical structure and solubility parameter difference between both components. Asphalt–polymer blends obtained using mechanical mixing are generally pseudo-binary mixtures of two immiscible phases, i.e. asphalt-rich phase and polymer-rich phase. To obtain modified binders with good road performance, small size, regular shape and good dispersion of polymer particles are required. In this study, the polymers used to modify the asphalt can be divided into two groups: the first group of non-grafted polymers forms a physical network swollen by the asphalt (maltene fraction), while the latter group is grafted with MAH and it may likely cross-link and/or chemically bond with the molecules of asphaltenes. SBS, SIS and SEBS are polymers that exhibit physical cross-linking; they have a two-phase morphology consisting of glassy micro-domains made of PS connected by mid-block (butadiene, isoprene or ethylene/butylene) segments. They maintain their micro-structure and are able to confer elastomeric properties to the whole material without losing melt processability at high temperatures. There is better dispersion of polymer in the micrograph of modified asphalt with SIS (Figure 2(e)) compared with the samples modified with SBS (Figure 2 (a)) and SEBS (Figure 2(c)), in which the light areas are larger and longer. Thus, it is possible to infer that for the mix conditions used here, the SIS is better dispersed than the linear SBS and SEBS due to a more favoured interaction between the SIS structure and the maltene fraction. In the SBS and SIS copolymers, the polarity of the aromatic rings of the PS blocks and the double bonds in mid-block sequences have a strong affinity with the aromatic and resin fractions of the asphalt. SEBS is considerably less polar than SBS and SIS, and it is relatively miscible with maltenes, although almost completely immiscible with asphaltenes. The net result of SBS hydrogenation is a lower compatibility with the asphalt, and this is perhaps the main reason why the use of SEBS as a modifier for road paving binders is presently rather limited. SIS/asphalt blend should be more stable under high-temperature storage conditions than the SBS and SEBS-modified asphalts (Table 2). An even better homogeneity of the shape and distribution of the light areas were observed for the grafted polymers, showing that they affect the interaction or compatibility between the polymer and asphalt binder. For instance, the fluorescence photomicrograph of the SBS-modified asphalt binder presents poor phase dispersion (Figure 2(a)), with coarse elastomer particles, while the asphalt/SBS-g-MAH blend presents a reduction in the size of polymer particles but it is not well dispersed, indicating that the addition of MAH to SBS (0.4 wt%) had a weaker influence (Figure 2 (b)). Although the SBS-g-MAH shows a slight improved morphology, this system is unstable under high-temperature storage conditions. The SEBS-modified asphalt shows poor phase dispersion, with coarse elastomer particles (Figure 2(c)). The blend has large polymer-rich islands that are not spherical but appear much more irregular and again contain internal black spots. The SEBS-g-MAH blend shows an improved morphology, attributed to a better interaction between the polar groups of polymer (MAH) and asphaltenes (Figure 2(d)), thus making the composition a very important parameter (Giuliani *et al.* 2009). More experimental data are required here to validate these conclusions. Either the two phases are more continuous or they may form two interlocked continuous phases with network structure, which may result in a large increase in binder properties. The fluorescence microscope image for SIS polymer contains small spherical shapes of polymer

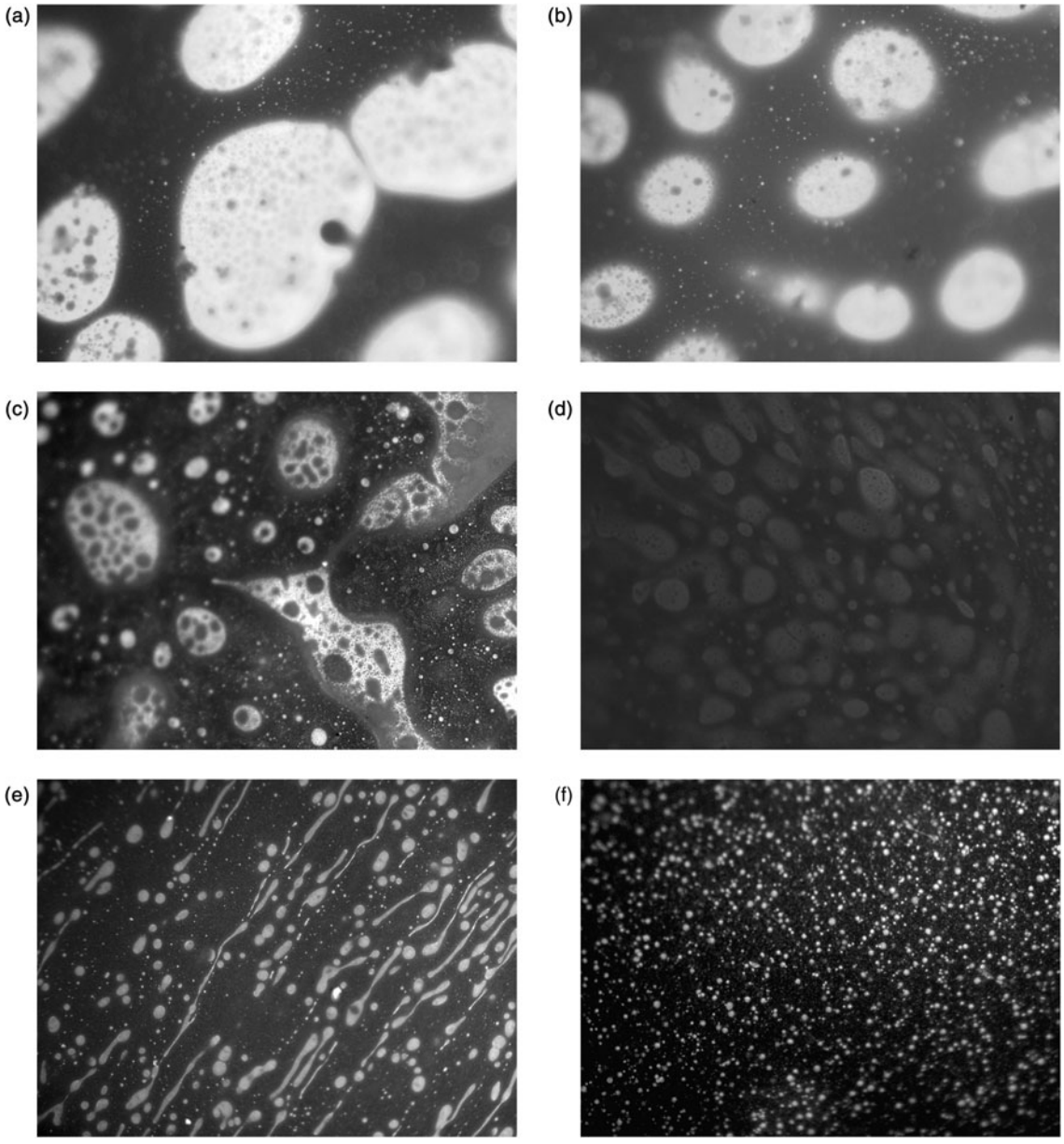

Figure 2. Fluorescence micrographs of modified asphalt binder with 20 × magnification: (a) asphalt/SBS, (b) asphalt/SBS-g-MAH, (c) asphalt/SEBS, (d) asphalt/SEBS-g-MAH, (e) asphalt/SIS and (f) asphalt/SIS-g-MAH.

dispersed in the asphalt (Figure 2(e)). Better result in the fluorescence analysis is observed in the SIS-g-MAH blend (Figure 2(f)). Its particle size is very small and dispersion in the asphalt matrix is very good, implying that this binder promoted a more effective polymer network in the asphalt and larger temperature storage stability (see Table 2). The addition of grafted tri-block polymers may form a more perfect network in the modified asphalt binder.

4.4 *Storage stability tests*

One of the most critical aspects of asphalt modification is storage stability, which is highly different for the non-grafted and grafted polymers. As far as thermodynamic stability is concerned, the compatibility between the polymer and the base asphalt is reflected in a uniform distribution in the blend (see Section 4.3). Under storage at high temperature, phase separation may occur depending on the particle size, density and viscosity differences between the polymer and the asphalt (Wen *et al.* 2002). Migration of the polymer droplets to the upper part of the test tube, while the asphalt remains in the lower part, is indicative of phase separation. Differences in the softening temperature between the lower and upper parts of the test tube determine the stability of the blend. Effects of the grafted polymer on storage stability of the modified

asphalt are shown in Table 2. Obviously, for asphalt modified with non-grafted polymers, the difference in the softening points is large, implying phase separation. According to the usual rule, the difference in the softening points should not be larger than 2.5°C. Therefore, the non-grafted polymer/asphalt blend is not recommended in pavements, while the modified asphalt with grafted polymers shows better compatibility, especially with SIS-g-MAH.

Grafted polymers have polar groups, which may form chemical bonds between the polymer and asphalt to prevent phase separation after the curing process or under thermal stability tests. The reaction occurs not only through the single Diels–Alder mechanism, alternating copolymerisation or charge transfer, but also through the mutual combination. Although the reaction of asphalt and MAH has been studied to obtain better paving performances, the reaction mechanism is still unclear (Kang *et al.* 2010). Herrington *et al.* (1999) proposed that the most likely reaction route is a Diels–Alder reaction involving the active MAH double bond and condensed aromatic ring systems in the asphalt. Because the anhydride ring opens during the reaction, the final result is the introduction of two carboxylic acid sites into the asphalt molecule. The new acid groups are able to hydrogen bond to polar groups on other asphalt molecules, giving rise to the observed changes in physical properties discussed earlier.

PMAs may be considered as a suspension system, where the particles in the liquid experience buoyancy and gravitational forces. The sedimentation velocity of the particles in the system follows Stoke's law (Ouyang *et al.* 2005):

$$V = \frac{2(\rho_0 - \rho_1)gr^2}{9\eta}, \tag{15}$$

where ρ_0 is the density of asphalt, ρ_1 is the density of polymer, g is the gravitational force constant, r is the average radius of the polymer particles and η is the viscosity of the modified asphalt. To prevent phase separation, a reduction in the sedimentation velocity is necessary, and this is achieved by a reduction in the particle size, increasing the viscosity or decreasing the density difference. Grafted polymers have active functional groups, creating strong interactions between asphalt and polymer, and thus phase separation is prevented due to induced high viscosity and small particle size in this case.

On the other hand, absorbance and swelling change the colloidal structure of asphalt, improving interfacial properties between polymer and base asphalt. Better absorbance, swelling and a thicker interfacial layer are sought. The properties of the interface layer, especially the cohesive strength and the thickness, have a substantial effect on the hot storage stability of PMA. A low cohesive strength and a thin interface layer indicate that the interfacial tension force between polymer and asphalt is high, inducing instability in the interface layer and further separation. Hence, the grafted polymer-modified asphalts with a stable interface layer have good high-temperature storage stability. Obviously, the smaller particles (as those of the SIS-g-MAH blend) possess large surface area, and thus small particles together with an increase in thickness and cohesive strength of the interface layer are advantageous to the storage stability; this should be achieved by chemical modification of the asphalt, because chemical adsorption is far stronger than physical adsorption. The interface layer maintained by physical and chemical adsorption is stable and is not easily destroyed by thermal agitation. The thickness of the interface between the two polymers depends on the product of the average molecule weight of the mixture and the square of the difference of solubility parameter of the two phases: $M^*(\delta_1-\delta_2)^2$. When the difference between δ_1 and δ_2 is relatively large, decreasing diffusion of the two phases across the interface results in a thin interface. When the difference between δ_1 and δ_2 is relatively small, the system tends to be a homogeneous phase system due to a thicker interface (Peng *et al.* 2002).

The storage stability was evaluated by the separation index I_S, defined according to the following expression (Lu and Isacsson 1997):

$$I_S = \log \frac{G^*_{\text{BOTTOM-PHASE}}}{G^*_{\text{TOP-PHASE}}}, \tag{16}$$

where G^* is the complex modulus. I_S is calculated at 25°C with 10 rad/s frequency.

Values of this index are shown in Table 2, revealing that the blends prepared with the grafted polymers are more stable than those prepared with the non-grafted compounds (lower I_S values). It is important to point out that the softening temperature data are irrelevant when applied to highly elastic blends. In the stability test, the elasticity of the upper section may be larger while that of the bottom becomes more rigid.

4.5 *Rheological properties*

A specific test method is used to determine the shear resistance of asphalt binders at temperatures at which rutting occur (AASHTO T 315). The point when $|G^*|/\sin\delta$ attains 1 kPa at 10 rad/s defines the maximum temperature for a good viscoelastic performance of the original binder once in the pavement (T_{SHRP}). To define the maximum pavement temperature, the analysis related to ageing of the rolling thin film oven (RTFO) asphalt binder is needed. Blends display higher temperatures than those of asphalt and the presence of MAH increases even more than this temperature (see Table 3). It is apparent that the modified asphalt prepared with grafted polymers has

Table 3. Parameter SHRP, activation energies, and slopes of G' and G'' in the terminal region for the blends.

Material	T_{SHRP} 10 rad/s (°C)	E_a (kJ/mol)	$(dG'/d\omega)_{\omega\to 0}$	$(dG''/d\omega)_{\omega\to 0}$
Asphalt	67	160	1.80	0.96
Asphalt/SBS	74	170	1.46	0.86
Asphalt/SBS-g-MAH	80	175	1.21	0.80
Asphalt/SIS	82	173	1.15	0.83
Asphalt/SIS-g-MAH	89	180	0.86	0.70
Asphalt/SEBS	83	172	1.40	0.98
Asphalt/SEBS-g-MAH	87	178	1.30	0.94

higher rutting resistance than that prepared with partner polymers. Consequently, the in-service temperature of the grafted polymer–asphalt blend is enhanced, improving road performance.

The dynamic viscosity $\eta'(\omega)$ of the asphalt and blends at 75°C is shown in Figure 3. Newtonian behaviour dominates throughout the frequency range. In contrast, asphalt/SIS-g-MAH deviates from this behaviour, because viscosity increases at low frequency. In this region, the dynamic viscosity of this blend is almost one and a half decade larger than that of the asphalt, while at high frequencies ($\omega = 100$ rad/s), η' is close to that of the asphalt. At low frequency, the increase in the viscosity is related to increased polymer–asphalt interactions, while at high frequency the effect of entanglements dominates. The observed behaviour reveals that although interactions are increased, the degree of entanglements is similar in the grafted and non-grafted samples.

In general, asphalt is considered as a thermo-rheological complex material in the linear viscoelastic range (Lesueur and Gerard 1996). To test time–temperature superposition, master curves were constructed for the linear viscoelastic properties as a function of frequency for various temperatures. The shifting factor a_T follows nearly Arrhenius-like temperature dependence, i.e. (Navarro *et al.* 2001, 2002, 2007):

$$a_T = \exp\left[\frac{E_a}{R}\left(\frac{1}{T} - \frac{1}{T_0}\right)\right], \tag{17}$$

where T_0 is the reference temperature (298 K) and E_a is the activation energy. Activation energies are disclosed in Table 3. E_a increases in the grafted samples, especially for the SIS-g-MAH system. These values are similar to those reported in the current literature for asphalts and PMA (Navarro *et al.* 2001, 2007). Higher activation energies are

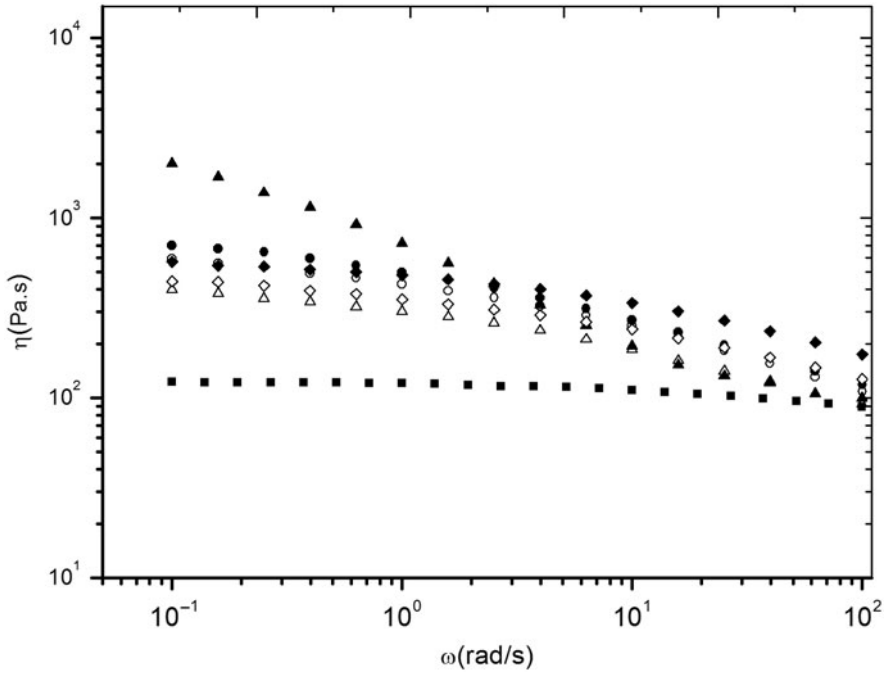

Figure 3. Dynamic viscosity $\eta'(\omega)$ for asphalt and blends at $T = 75$°C. (■) asphalt; (○) SBS; (●) SBS-g-MAH; (△) SIS; (▲) SIS-g-MAH; (◇) SEBS; (◆) SEBS-g-MAH.

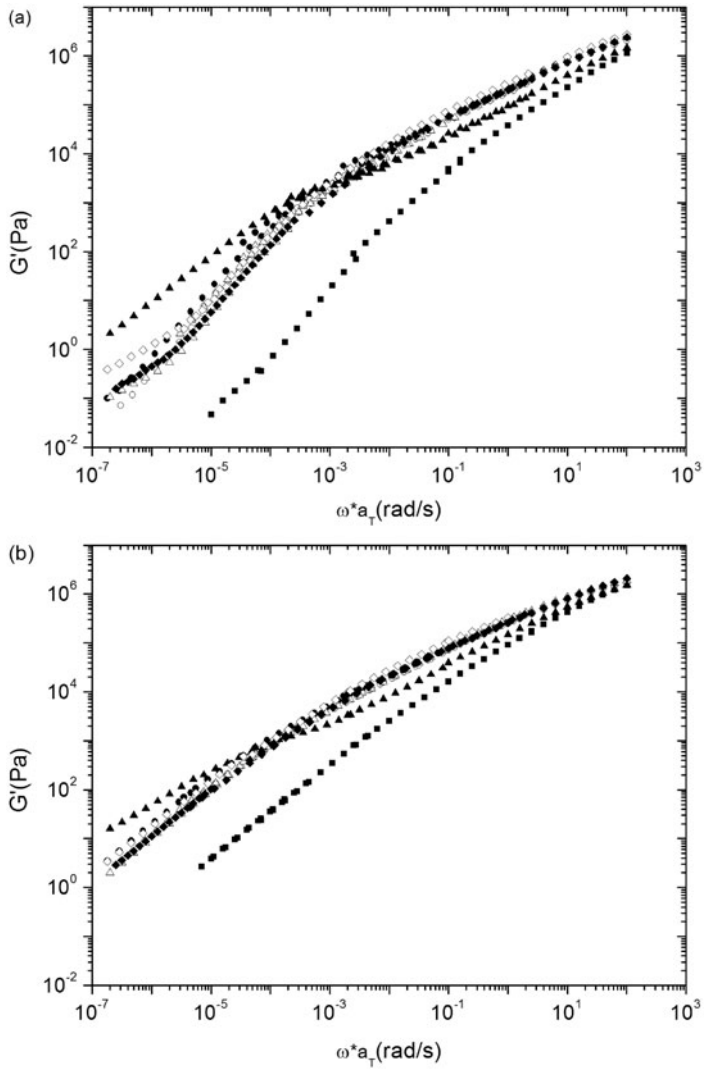

Figure 4. Master curves: (a) storage modulus, and (b) loss modulus for asphalt and blends, obtained using frequency–temperature superposition method and a reference temperature $T = 25$°C. a_T is the shift factor that accounts for the frequency–temperature equivalence. (■) asphalt; (○) SBS; (●) SBS-g-MAH; (△) SIS; (▲) SIS-g-MAH; (◇) SEBS; (◆) SEBS-g-MAH.

related to a larger energy barrier to flow, and this is normally observed in more complex polymer systems.

The rheological characterisation allows building master curves from the dynamic data taken in isothermal frequency sweep tests. The TTSP was found to hold for all the materials and the horizontal shifting factor was satisfactorily described by the Arrhenius dependence. Master curves of the storage modulus (G') and loss modulus (G'') as functions of reduced frequency ($\omega^* a_T$) for asphalt and the blends are shown in Figure 4(a)–(b). As the asphalt is modified, an increase in G' is observed at low frequency or terminal region corresponding to the viscoelastic behaviour at long times and high temperatures. Also, G' is lower than G'', and the slopes are smaller than 2 and 1, respectively, for the blends with grafted polymers (Table 3). A deviation from the Maxwell behaviour is characteristic for these materials, where the asphalt/SIS-g-MAH presents the smallest slope among the systems studied. In addition, G' of this blend is approximately one and a half decade larger than the asphalt value, while the other blends present values of one decade larger. At intermediate reduced frequency (1.4×10^{-5}–3×10^{-3} rad/s), the asphalt/SIS-g-MAH blend shows a slope change or slight tendency to a plateau that may be related to the branching of the SIS copolymer, while the other blends present similar values of G'. An increase in the elastic and viscous moduli in the high in-service temperatures range improves the rutting resistance property of the resulting pavement. The observed rheological behaviour is a consequence of the presence of rubber particles swollen by light components of the maltene fraction or by the formation or enhancement of transient networks of asphalt species, linked by hydrogen bonding and dipole–dipole interactions (Herrington *et al.* 1999).

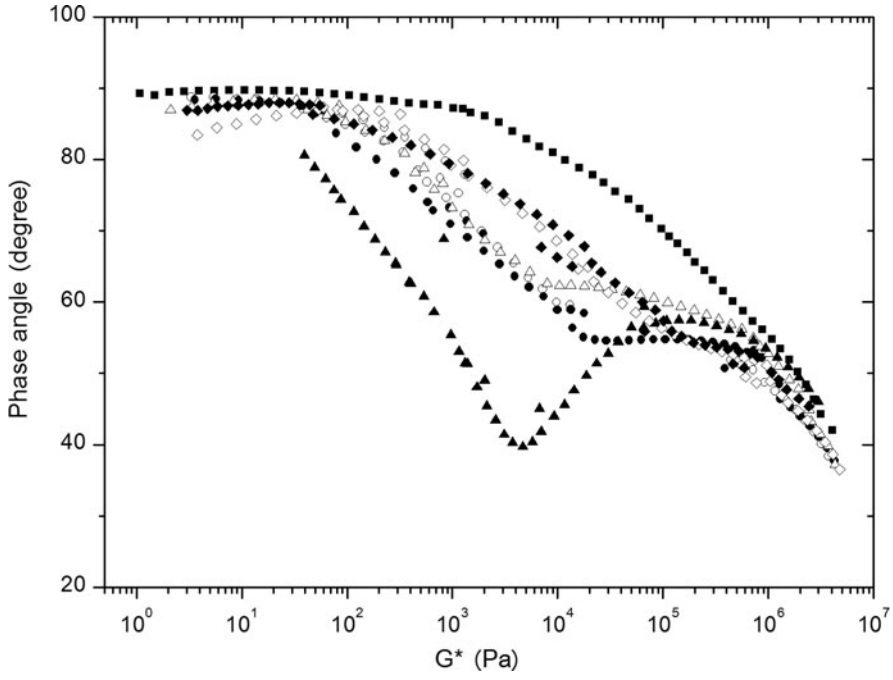

Figure 5. Black diagrams of rheological data for asphalt and blends. (■) asphalt; (○) SBS; (●) SBS-g-MAH; (△) SIS; (▲) SIS-g-MAH; (◇) SEBS; (◆) SEBS-g-MAH.

The range of superposition was tested by Black diagrams construction, δ versus $|G^*|$ (Figure 5). Curves for the blends are different to that of asphalt caused by the presence of the modifying polymer (Airey *et al.* 2003, Polacco *et al.* 2006). The shape of the curves for asphalt with SBS, SEBS and SIS is characteristic of a behaviour related to increased elasticity (low values of the phase angle δ) while that of the asphalt/SIS-g-MAH is 'stretched out' by the addition of MAH. Changes in the shape of the black curve from a broad S-like curve (typical for heavily modified elastomeric binders) to a very narrow S-like curve upon MAH addition (SIS-g-MAH) are observed. This is due to the modification in the breath of the relaxation time spectrum by grafting. Asphalt modification by polymers is mainly manifested at elevated temperatures, while low-temperature behaviour is known to be less influenced by polymer modifiers (Polacco *et al.* 2004a).

The curves of all systems are superposed over the range of temperature analysed; this suggests that the materials show thermo-simplicity and the TTSP is valid. Others authors have found that the TTSP holds for other materials such as SEBS (Polacco *et al.* 2006) and SBS (Airey *et al.* 2003, Navarro *et al.* 2005, 2009), and even for reactive polymers (RET), e.g. ethylene–butylacrylate–glycidylmethacrylate (Polacco *et al.* 2004a), MAH functionalised polyethylene (Da Silva *et al.* 2004) and so on.

On the basis of experimental evidence, the grafting degree of the MAH in SBS, SIS or SEBS has an effect on the rheological properties, thermal stability and compatibility of the modified asphalt. Modified asphalts were improved in the following order: SBS-g-MAH < SEBS-g-MAH < -SIS-g-MAH. The difference between SBS-g-MAH and SIS-g-MAH should be due to MAH content, structure of the base polymer and molecular weight (Table 1). The presence of a chemical bond within the polymer and asphaltenes strongly reduces phase separation, while radial structure of SIS-g-MAH should favour network formation. In addition, SEBS-g-MAH decreases the crystallinity content in the polymer (Passaglia *et al.* 2000) and improves the grafting reaction. This in turn improves the thermal stability and compatibility (via reactions between functional groups of asphalt and MAH groups of the polymer) but not the mechanical properties. SEBS-g-MAH polymers should only be used if the network formed is kept below the 'chemical' gel point.

4.6 *Fractional models*

Predictions with fractional models over a range of frequencies at various temperatures are described in this section, using a minimum number of parameters for asphalt and blends. These materials are evaluated using three fractional models: FMM, FKM and FSLS. A comparison between the parameters obtained in the models used in the predictions of the experimental data for asphalt and blends are shown in Tables 4–6.

Storage (G') and loss moduli (G'') of asphalt and blends were calculated using FMM, Equations (4) and (5). FMM

Table 4. FMM parameters at different temperatures.

Material	75°C $\omega = 0.1–100$ rad/s	60°C $\omega = 0.1–100$ rad/s	40°C $\omega = 0.1–100$ rad/s	25°C $\omega = 0.1–100$ rad/s
Asphalt	$\eta = 4.1 \times 10^5$ Pa s $\alpha = 0.99$; $\tau_R = 8$ s	$\eta = 3.86 \times 10^5$ Pa s $\alpha = 0.98$; $\tau_R = 1.7$ s	$\eta = 1.7 \times 10^5$ Pa s $\alpha = 0.89$; $\tau_R = 3 \times 10^{-2}$ s	$\eta = 1.5 \times 10^5$ Pa s $\alpha = 0.78$; $\tau_R = 1 \times 10^{-5}$ s
Asphalt/SBS	$\eta = 8 \times 10^6$ Pa s $\alpha = 0.93$; $\tau_R = 5$ s	$\eta = 8.7 \times 10^5$ Pa s $\alpha = 0.77$; $\tau_R = 2.3$ s	$\eta = 4.2 \times 10^5$ Pa s $\alpha = 0.65$; $\tau_R = 1.2$ s	$\eta = 3.5 \times 10^5$ Pa s $\alpha = 0.6$; $\tau_R = 0.1$ s
Asphalt/SBS-g-MAH	$\eta = 8 \times 10^6$ Pa s $\alpha = 0.91$; $\tau_R = 1.5$ s	$\eta = 2 \times 10^6$ Pa s $\alpha = 0.8$; $\tau_R = 0.5$ s	$\eta = 4.5 \times 10^5$ Pa s $\alpha = 0.62$; $\tau_R = 0.1$ s	$\eta = 4 \times 10^5$ Pa s $\alpha = 0.6$; $\tau_R = 0.09$ s
Asphalt/SIS	$\eta = 2.0 \times 10^6$ Pa s $\alpha = 0.88$; $\tau_R = 2.0$ s	$\eta = 1.08 \times 10^6$ Pa s $\alpha = 0.8$; $\tau_R = 1$ s	$\eta = 4.5 \times 10^5$ Pa s $\alpha = 0.7$; $\tau_R = 0.8$ s	$\eta = 4.2 \times 10^5$ Pa s $\alpha = 0.67$; $\tau_R = 0.16$ s
Asphalt/SIS-g-MAH	$\eta = 2.5 \times 10^6$ Pa s $\alpha = 0.62$; $\tau_R = 25$ s	$\eta = 5.1 \times 10^5$ Pa s $\alpha = 0.58$; $\tau_R = 10$ s	$\eta = 1.45 \times 10^5$ Pa s $\alpha = 0.56$; $\tau_R = 0.1$ s	$\eta = 1.25 \times 10^5$ Pa s $\alpha = 0.52$; $\tau_R = 0.03$ s
Asphalt/SEBS	$\eta = 5.0 \times 10^6$ Pa s $\alpha = 0.93$; $\tau_R = 28$ s	$\eta = 3.5 \times 10^6$ Pa s $\alpha = 0.89$; $\tau_R = 1.5$ s	$\eta = 5.0 \times 10^5$ Pa s $\alpha = 0.74$; $\tau_R = 0.1$ s	$\eta = 5 \times 10^5$ Pa s $\alpha = 0.63$; $\tau_R = 0.06$ s
Asphalt/SEBS-g-MAH	$\eta = 6 \times 10^6$ Pa s $\alpha = 0.9$; $\tau_R = 15$ s	$\eta = 3 \times 10^6$ Pa s $\alpha = 0.87$; $\tau_R = 0.3$ s	$\eta = 7 \times 10^5$ Pa s $\alpha = 0.7$; $\tau_R = 0.1$ s	$\eta = 3.5 \times 10^5$ Pa s $\alpha = 0.57$; $\tau_R = 0.06$ s

describes appropriately these moduli from 75 to 25°C at frequencies of 0.1–100 rad/s in all samples with only three parameters (Table 4). In general, viscosity, fractional order and relaxation time decrease as the temperature diminishes in all systems. These parameters are higher in modified asphalt than those of neat asphalt and increase slightly in the grafted blends but no discernible tendency is observed among the grafted polymers. Asphalt/SIS and asphalt/SIS-g-MAH present lower fractional order (α) at 75°C than the other systems (0.88 and 0.62, respectively), revealing an elastic behaviour. The parameter α changes from 0.93 to 0.52 in the blends (tendency to elastic behaviour), while that for the asphalt presents a viscous behaviour as $\alpha \rightarrow 1$ at high temperature.

The corresponding parameters used in the FKM model (Equations (8) and (9)) are shown in Table 5. Agreement is fairly good from 75 to 25°C at 0.1–100 rad/s for the storage and loss modulus. Same behaviour of viscosity and fractional order is observed with respect to FMM, while G_∞ is practically constant at all temperatures and samples. The viscosity obtained in both models is of the same order of magnitude, while α presents slight differences. This model is sensitive only to viscosity and fractional order.

The moduli G' and G'' were calculated using the four-parameter FSLS model through Equations (12) and (13), with parameters given in Table 5. The FSLS model represents well the data throughout the temperature range. Viscosity and fractional order decrease as the temperature diminishes, while G_d and G_0 are practically constant. The additional spring in series G_d with a value of 1.0×10^{-2} ($G_d \rightarrow 0$) implies a reduction in FSLS to FMM. Fractional order and viscosity are of the same order of magnitude than that of FMM and FKM. Substantial differences were not found between the three models used in this work.

5. Conclusions

The modified asphalt with the grafted polymers shows an increase in the softening temperature and diminishing penetration, due to an increase in rigidity. From the fluorescence analysis, it is possible to infer that grafted polymers improve the morphology and interaction between the mixture components while the partner polymers (SBS and SEBS) present a poor polymer distribution. The grafted copolymers induce a deviation from Maxwellian behaviour at low frequencies (lower slopes of G' and G'', revealing increased interactions). A slight tendency to a plateau is observed in the asphalt/SIS-g-MAH blend master curve, which should be related to the branching of the SIS copolymer. On the basis of experimental evidence, the MAH grafting causes an increase in the elastic behaviour of the blends and dynamic viscosity. The activation energy of asphalt increases with polymer addition, even in the blends prepared with MAH-functionalised polymers. The observed master curves validate temperature superposition principle for asphalt and blends.

Larger values of ($G^*/\sin\delta$) demonstrates that the asphalt blends prepared with the SIS-g-MAH may be less sensitive to permanent deformation. The enhancement of blend properties observed by grafted polymer may be a consequence of chemical reactions between MAH groups of the reactive polymer with polar groups of asphalt. Unfortunately, due to the extremely complex chemical nature and composition of asphalts, it is difficult to detect the real nature of chemical bonds formed during the processing and thermal storage test.

On the other hand, the results obtained demonstrate that the non-grafted PMA samples are largely unstable during storage at high temperature, while grafted polymers

Table 5. FKM parameters used at different temperatures.

Material	75°C $\omega = 0.1–100$ rad/s	60°C $\omega = 0.1–100$ rad/s	40°C $\omega = 0.1–100$ rad/s	25°C $\omega = 0.1–100$ rad/s
Asphalt	$\eta = 1.2 \times 10^6$ Pa s $\alpha = 0.99$; $G_\infty = 1 \times 10^{-1}$ Pa	$\eta = 8.6 \times 10^5$ Pa s $\alpha = 0.96$; $G_\infty = 1 \times 10^{-1}$ Pa	$\eta = 1.9 \times 10^5$ Pa s $\alpha = 0.88$; $G_\infty = 1 \times 10^{-1}$ Pa	$\eta = 1.4 \times 10^5$ Pa s $\alpha = 0.6$; $G_\infty = 1 \times 10^{-1}$ Pa
Asphalt/SBS	$\eta = 7.4 \times 10^6$ Pa s $\alpha = 0.92$; $G_\infty = 1 \times 10^{-1}$ Pa	$\eta = 1.1 \times 10^6$ Pa s $\alpha = 0.82$; $G_\infty = 1 \times 10^{-1}$ Pa	$\eta = 4.7 \times 10^5$ Pa s $\alpha = 0.70$; $G_\infty = 1 \times 10^{-1}$ Pa	$\eta = 2.8 \times 10^5$ Pa s $\alpha = 0.58$; $G_\infty = 1 \times 10^{-1}$ Pa
Asphalt/SBS-g-MAH	$\eta = 8.4 \times 10^6$ Pa s $\alpha = 0.9$; $G_\infty = 1 \times 10^{-1}$ Pa	$\eta = 2.1 \times 10^6$ Pa s $\alpha = 0.80$; $G_\infty = 1 \times 10^{-1}$ Pa	$\eta = 5.6 \times 10^5$ Pa s $\alpha = 0.67$; $G_\infty = 1 \times 10^{-1}$ Pa	$\eta = 3.0 \times 10^5$ Pa s $\alpha = 0.55$; $G_\infty = 1 \times 10^{-1}$ Pa
Asphalt/SIS	$\eta = 2.1 \times 10^6$ Pa s $\alpha = 0.84$; $G_\infty = 1 \times 10^{-1}$ Pa	$\eta = 1.0 \times 10^6$ Pa s $\alpha = 0.77$; $G_\infty = 1 \times 10^{-1}$ Pa	$\eta = 4.3 \times 10^5$ Pa s $\alpha = 0.68$; $G_\infty = 1 \times 10^{-1}$ Pa	$\eta = 3.6 \times 10^5$ Pa s $\alpha = 0.55$; $G_\infty = 1 \times 10^{-1}$ Pa
Asphalt/SIS-g-MAH	$\eta = 2.1 \times 10^6$ Pa s $\alpha = 0.6$; $G_\infty = 1 \times 10^{-1}$ Pa	$\eta = 9.0 \times 10^5$ Pa s $\alpha = 0.48$; $G_\infty = 1 \times 10^{-1}$ Pa	$\eta = 2.5 \times 10^5$ Pa s $\alpha = 0.46$; $G_\infty = 1 \times 10^{-1}$ Pa	$\eta = 1.7 \times 10^5$ Pa s $\alpha = 0.42$; $G_\infty = 1 \times 10^{-1}$ Pa
Asphalt/SEBS	$\eta = 6.3 \times 10^6$ Pa s $\alpha = 0.92$; $G_\infty = 1 \times 10^{-1}$ Pa	$\eta = 1.2 \times 10^5$ Pa s $\alpha = 0.76$; $G_\infty = 1 \times 10^{-1}$ Pa	$\eta = 5.8 \times 10^5$ Pa s $\alpha = 0.64$; $G_\infty = 1 \times 10^{-1}$ Pa	$\eta = 3.8 \times 10^5$ Pa s $\alpha = 0.56$; $G_\infty = 1 \times 10^{-1}$ Pa
Asphalt/SEBS-g-MAH	$\eta = 5.7 \times 10^6$ Pa s $\alpha = 0.9$; $G_\infty = 1 \times 10^{-1}$ Pa	$\eta = 9.0 \times 10^5$ Pa s $\alpha = 0.76$; $G_\infty = 1 \times 10^{-1}$ Pa	$\eta = 3.5 \times 10^5$ Pa s $\alpha = 0.60$; $G_\infty = 1 \times 10^{-1}$ Pa	$\eta = 2.7 \times 10^5$ Pa s $\alpha = 0.56$; $G_\infty = 1 \times 10^{-1}$ Pa

Table 6. FSLS parameters used for asphalt and blends at different temperatures.

Material	75°C $\omega = 0.1–100$ rad/s	60°C $\omega = 0.1–100$ rad/s	40°C $\omega = 0.1–100$ rad/s	25°C $\omega = 0.1–100$ rad/s
Asphalt	$\eta = 4.0 \times 10^5$ Pa s $\alpha = 0.99$; $G_0 = 7 \times 10^4$ Pa; $G_d = 1 \times 10^{-2}$ Pa	$\eta = 2.0 \times 10^5$ Pa s $\alpha = 0.96$; $G_0 = 6.0 \times 10^4$ Pa; $G_d = 1 \times 10^{-2}$ Pa	$\eta = 9.6 \times 10^4$ Pa s $\alpha = 0.86$; $G_0 = 6 \times 10^4$ Pa; $G_d = 1 \times 10^{-2}$ Pa	$\eta = 6.5 \times 10^4$ Pa s $\alpha = 0.68$; $G_0 = 5 \times 10^4$ Pa; $G_d = 1 \times 10^{-2}$ Pa
Asphalt/SBS	$\eta = 8.5 \times 10^6$ Pa s $\alpha = 0.93$; $G_0 = 7 \times 10^7$ Pa; $G_d = 1 \times 10^{-2}$ Pa	$\eta = 1.2 \times 10^6$ Pa s $\alpha = 0.81$; $G_0 = 5.0 \times 10^7$ Pa; $G_d = 1 \times 10^{-2}$ Pa	$\eta = 3.7 \times 10^5$ Pa s $\alpha = 0.63$; $G_0 = 5 \times 10^7$ Pa; $G_d = 1 \times 10^{-2}$ Pa	$\eta = 2.7 \times 10^5$ Pa s $\alpha = 0.58$; $G_0 = 5 \times 10^7$ Pa; $G_d = 1 \times 10^{-2}$ Pa
Asphalt/SBS-g-MAH	$\eta = 8 \times 10^6$ Pa s $\alpha = 0.9$; $G_0 = 5 \times 10^7$ Pa; $G_d = 1 \times 10^{-2}$ Pa	$\eta = 2.0 \times 10^6$ Pa s $\alpha = 0.8$; $G_0 = 1.0 \times 10^7$ Pa; $G_d = 1 \times 10^{-2}$ Pa	$\eta = 5.8 \times 10^5$ Pa s $\alpha = 0.67$; $G_0 = 5 \times 10^7$ Pa; $G_d = 1 \times 10^{-2}$ Pa	$\eta = 3.0 \times 10^5$ Pa s $\alpha = 0.56$; $G_0 = 5 \times 10^7$ Pa; $G_d = 1 \times 10^{-2}$ Pa
Asphalt/SIS	$\eta = 3 \times 10^6$ Pa s $\alpha = 0.9$; $G_0 = 5 \times 10^7$ Pa; $G_d = 1 \times 10^{-2}$ Pa	$\eta = 1.2 \times 10^6$ Pa s $\alpha = 0.82$; $G_0 = 5.0 \times 10^7$ Pa; $G_d = 1 \times 10^{-2}$ Pa	$\eta = 5 \times 10^5$ Pa s $\alpha = 0.7$; $G_0 = 5 \times 10^7$ Pa; $G_d = 1 \times 10^{-2}$ Pa	$\eta = 3.5 \times 10^5$ Pa s $\alpha = 0.56$; $G_0 = 5 \times 10^7$ Pa; $G_d = 1 \times 10^{-2}$ Pa
Asphalt/SIS-g-MAH	$\eta = 2.5 \times 10^6$ Pa s $\alpha = 0.6$; $G_0 = 5 \times 10^7$ Pa; $G_d = 1 \times 10^{-2}$ Pa	$\eta = 1.2 \times 10^5$ Pa s $\alpha = 0.56$; $G_0 = 5.0 \times 10^7$ Pa; $G_d = 1 \times 10^{-2}$ Pa	$\eta = 1.2 \times 10^5$ Pa s $\alpha = 0.54$; $G_0 = 5 \times 10^7$ Pa; $G_d = 1 \times 10^{-2}$ Pa	$\eta = 1.5 \times 10^5$ Pa s $\alpha = 0.5$; $G_0 = 5 \times 10^7$ Pa; $G_d = 1 \times 10^{-2}$ Pa
Asphalt/SEBS	$\eta = 7.6 \times 10^6$ Pa s $\alpha = 0.92$; $G_0 = 5 \times 10^7$ Pa; $G_d = 1 \times 10^{-2}$ Pa	$\eta = 2.6 \times 10^6$ Pa s $\alpha = 0.84$; $G_0 = 5.0 \times 10^7$ Pa; $G_d = 1 \times 10^{-2}$ Pa	$\eta = 4.6 \times 10^5$ Pa s $\alpha = 0.6$; $G_0 = 5 \times 10^7$ Pa; $G_d = 1 \times 10^{-2}$ Pa	$\eta = 4 \times 10^5$ Pa s $\alpha = 0.56$; $G_0 = 5 \times 10^7$ Pa; $G_d = 1 \times 10^{-2}$ Pa
Asphalt/SEBS-g-MAH	$\eta = 6 \times 10^6$ Pa s $\alpha = 0.9$; $G_0 = 5 \times 10^7$ Pa; $G_d = 1 \times 10^{-2}$ Pa	$\eta = 2.2 \times 10^6$ Pa s $\alpha = 0.85$; $G_0 = 5 \times 10^7$ Pa; $G_d = 1 \times 10^{-2}$ Pa	$\eta = 4 \times 10^5$ Pa s $\alpha = 0.62$; $G_0 = 5 \times 10^7$ Pa; $G_d = 1 \times 10^{-2}$ Pa	$\eta = 3 \times 10^5$ Pa s $\alpha = 0.56$; $G_0 = 5 \times 10^7$ Pa; $G_d = 1 \times 10^{-2}$ Pa

enhance the storage stability. The grafting content of MAH in SBS, SIS or SEBS improves slightly the rheological properties, thermal stability and compatibility of the modified asphalt in the following order: SBS-g-MAH < SEBS-g-MAH < SIS-g-MAH.

The use of fractional models describes the viscoelasticity behaviour of the systems at different temperatures in the range of frequencies from 0.1 to 100 rad/s. Among the parameters obtained for the three models, viscosity and fractional order are similar. The parameter G_∞ of the FKM model is not sensitive to changes in temperature or frequency, while the parameter G_d of the FSLS model is practically constant.

Last but not the least, PMA must be cost-effective, which means that the high polymer cost must be balanced by both improved asphalt properties and the reduction in road maintenance and resurfacing costs. The chemical modification by polymers not only produces enhanced storage stability but also improves other properties. Several research teams around the world have worked on evaluating the benefits of polymer modification on pavement performance, and tests and specifications for binders are continuously being developed. Studies point out that, for optimal savings, it is desirable to choose an asphalt modifier that resists multiple distresses, such as rutting, fatigue, thermal cracking and water damage.

References

Aimin, Z. and Chao, L., 2003. Chemical initiation mechanism of maleic anhydride grafted onto styrene–butadiene–styrene block copolymer. *European Polymer Journal*, 39, 1291–1295.

Airey, G.D., Mohammed, M.H., and Fichter, C., 2008. Rheological characteristics of synthetic road binders. *Fuel*, 87, 1763–1775.

Airey, G.D., Rahimzadeh, B., and Collop, A.C., 2003. Viscoelastic linearity limits for bituminous materials. *Materials and Structures*, 36, 643–647.

Becker, Y., Muller, A.J., and Rodriguez, Y., 2003. Use of rheological compatibility criteria to study SBS modified asphalts. *Journal of Applied Polymer Science*, 90 (7), 1772–1782.

Brûle, B., 1996. Polymer-modified asphalt cements used in the road construction industry: basic principles. *Transportation Research Record*, Washington, DC: TRB, National Research Council, 1535–1543.

Brûle, B., Brion, Y., and Tanguy, A., 1988. Paving asphalt polymer blends: relationships between composition, structure and properties. *Proceedings of the Association of Asphalt Paving Technologists*, 57, 41–63.

Collins, J.H. and Bouldin, M.G., 1992. Long and short term stability of straight and polymer modified asphalts. *Rubber World*, 32–68.

Collins, J.H. and Mikols, W.J., 1985. Block copolymer modification of asphalt intended for surface dressing applications. *Proceedings of the Association of Asphalt Paving Technologists*, 54, 1–17.

Cong, P., Chen, S., and Chen, H., 2011. Preparation and properties of bitumen modified with the maleic anhydride grafted styrene–butadiene–styrene triblock copolymer. *Polymer Engineering and Science*, 51, 1273–1279.

Da Silva, L.S., *et al.*, 2004. Study of rheological properties of pure and polymer-modified Brazilian asphalt binders. *Journal of Materials Science*, 39, 539–546.

Dharmarajan, N., *et al.*, 1995. Compatibilized polymer blends of isotactic polypropylene and styrene–maleic anhydride copolymer. *Polymer*, 36 (20), 3849–3861.

Friedrich, C., 1991. Relaxation and retardation functions of the Maxwell model with fractional derivatives. *Rheologica Acta*, 30, 151–158.

Fu, H., *et al.*, 2007. Storage stability and compatibility of asphalt binder modified by SBS graft copolymer. *Construction and Building Materials*, 21, 1528–1533.

Giuliani, F., *et al.*, 2009. Effects of polymer modification on the fuel resistance of asphalt binders. *Fuel*, 88, 1539–1546.

Heinen, W., *et al.*, 1996. ^{13}C NMR study of the grafting of maleic anhydride onto polyethene, polypropene, and ethene–propene copolymers. *Macromolecules*, 29, 1151–1157.

Hernández Jiménez, A., Vinagre Jara, B., and Hernández Santiago, J., 2002. Relaxation modulus in the fitting of polycarbonate and poly(vinyl chloride) viscoelastic polymers by a fractional Maxwell model. *Colloid and Polymer Science*, 280, 485–489.

Herrington, P.R., Wu, Y., and Forbes, M.C., 1999. Rheological modification of bitumen with maleic anhydride and dicarboxylic acids. *Fuel*, 78, 101–110.

Heymans, N., 1996. Hierarchical models for viscoelasticity: dynamic behavior in the linear range. *Rheologica Acta*, 35, 508–519.

Heymans, N. and Bauwens, J.C., 1994. Fractal rheological models and fractional differential equations for viscoelastic behavior. *Rheologica Acta*, 33, 210–219.

Jiang, D.D. and Wilkie, C.A., 1997. Chemical initiation of graft copolymerization of methyl methacrylate onto styrene–butadiene block copolymer. *Journal of Polymer Science Part A: Polymer Chemistry*, 35, 965–973.

Kang, Y., Wang, F., and Chen, Z., 2010. Reaction of asphalt and maleic anhydride: kinetics and mechanism. *Chemical Engineering Journal*, 164, 230–237.

Kraus, G., 1982. Modification of asphalt by block polymers of butadiene and styrene. *Rubber Chemistry and Technology*, 55 (5), 1389–1402.

Kraus, G. and Rollmam, K.W., 1980. *Morphology and mechanical behavior of bitumens modified with butadiene–styrene block polymers*. Bartlesville, OK: Phillips Petroleum Company, Research and Development Report 8672-80.

Lesueur, D. and Gerard, J.F., 1996. A structure-related model to describe asphalt linear viscoelasticity. *Journal of Rheology*, 40 (5), 813–836.

Lewandowski, R. and Chorazyczewski, B., 2010. Identification of the parameters of the Kelvin–Voigt and the Maxwell fractional models, used to modeling of viscoelastic dampers. *Computers and Structures*, 88, 1–17.

Lu, X. and Isacsson, U., 1997. Rheological characterization of styrene–butadiene–styrene copolymer modified bitumens. *Construction and Building Materials*, 11 (1), 23–32.

Machado, A.V., Covas, J.A., and van Duin, M., 2001. Effect of polyolefin structure on maleic anhydride grafting. *Polymer*, 42, 3649–3655.

Moad, G., 1999. The synthesis of polyolefin graft copolymers by reactive extrusion. *Progress in Polymer Science*, 24, 81–142.

Mohammad, H.I., *et al.*, 2006. Rheological investigation of the influence of acrylate polymers on the modification of asphalt. *Journal of Applied Polymer Science*, 102, 3446–3456.

Mun, S. and Zi, G., 2010. Modeling the viscoelastic function of asphalt concrete using a spectrum method. *Mechanics of Time-Dependent Materials*, 14, 191–202.

Nakason, C., Kaesaman, A., and Supasanthitikul, P., 2004. The grafting of maleic anhydride onto natural rubber. *Polymer Testing*, 23, 35–41.

Navarro, F.J., *et al.*, 2001. Effect of processing variables on the linear viscoelastic properties of SBS–oil blends. *Polymer Engineering and Science*, 41 (12), 2216–2225.

Navarro, F.J., *et al.*, 2002. Rheological characteristics of ground tire rubber-modified bitumens. *Chemical Engineering Journal*, 89, 53–61.

Navarro, F.J., *et al.*, 2005. Effect of composition and processing on the linear viscoelasticity of synthetic binders. *European Polymer Journal*, 41, 1429–1438.

Navarro, F.J., *et al.*, 2007. Influence of processing conditions on the rheological behavior of crumb tire rubber-modified bitumen. *Journal of Applied Polymer Science*, 104, 1683–1691.

Navarro, F.J., *et al.*, 2009. Bitumen modification with reactive and non-reactive (virgin and recycled) polymers: a comparative analysis. *Journal of Industrial and Engineering Chemistry*, 15, 458–464.

Ouyang, C., *et al.*, 2005. Preparation and properties of styrene–butadiene–styrene copolymer/kaolinite clay compound and asphalt modified with the compound. *Polymer Degradation and Stability*, 87, 309–317.

Passaglia, E., *et al.*, 2000. Grafting of diethyl maleate and maleic anhydride onto styrene-*b*-(ethylene-*co*-1-butene)-*b*-styrene triblock copolymer (SEBS). *Polymer*, 41, 4389–4400.

Papoulia, K.D., *et al.*, 2010. Rheological representation of fractional order viscoelastic material models. *Rheologica Acta*, 49, 381–400.

Peng, Y., *et al.*, 2002. Application of the compatibility theory and the solubility parameter theory in SBS modification asphalt. *Petroleum Science and Technology*, 3&4, 367–376.

Polacco, G., *et al.*, 2004a. Rheology of asphalts modified with glycidylmethacrylate functionalized polymers. *Journal of Colloid and Interface Science*, 280, 366–373.

Polacco, G., *et al.*, 2004b. Temporary networks in polymer-modified asphalts. *Polymer Engineering and Science*, 44 (12), 2185–2193.

Polacco, G., *et al.*, 2006. Effect of composition on the properties of SEBS modified asphalts. *European Polymer Journal*, 42, 1113–1121.

Qiu, W., Endo, T., and Hirotsu, T., 2005. A novel technique for preparing of maleic anhydride grafted polyolefins. *European Polymer Journal*, 41, 1979–1984.

Rossikhin, Y.A. and Shitikova, M.V., 2001. Analysis of rheological equations involving more than one fractional parameters by the use of the simplest mechanical systems based on these equations. *Mechanics of Time-Dependent Materials*, 5, 131–175.

Sánchez Solís, A., *et al.*, 2000. On the properties and processing of polyethylene terephthalate/styrene–butadiene rubber blend. *Polymer Engineering and Science*, 40, 1216–1225.

Stastna, J., Zanzotto, L., and Ho, K., 1994. Fractional complex modulus manifested in asphalts. *Rheologica Acta*, 33, 344–354.

Vargas, M.A., *et al.*, 2009. Viscoelasticity of asphalts modified with SEBS copolymers functionalized with various amounts of maleic anhydride. *Rubber Chemistry and Technology*, 82 (2), 244–264.

Wen, G., *et al.*, 2002. Rheological characterization of storage-stable SBS-modified asphalts. *Polymer Testing*, 21, 295–302.